Faculty of Physics and Astronomy

University of Heidelberg

Bachelor thesis

in Physics

submitted by

Frederike Schmitz

born in Mönchengladbach

July 2010

Schottky Diagnostics at the Heavy Ion Cooler Storage Ring TSR

This bachelor thesis has been carried out by
Frederike Schmitz
at the
Max Planck Institute for Nuclear Physics
under the supervision of
Dr. Manfred Grieser and Prof. Dr. Andreas Wolf

Abstract

Schottky diagnostics at the heavy ion cooler storage ring TSR

Schottky diagnostics uses the noise of the beam current in an ion storage ring, called the Schottky noise, to determine beam properties such as the momentum spread and the beam energy. In this thesis, Schottky diagnostics as well as the characteristics of the Schottky pick-up were discussed in theory. In experiments, two different electrostatic pick-ups were used to verify the properties of the Schottky pick-up and the theory of Schottky diagnostics. For the experiments, a $^{12}C^{6+}$ ion beam with an energy of 50 MeV was used. Signal distortions like amplification with a preamplifier and damping of the signal through long cables must be taken into account when analyzing the data. Hence, the frequency responses of the utilized amplifiers and cables were measured and used to adjust the recorded signals. The experimental data was compared to the theoretical expectations. Conclusions were drawn to model a new Schottky pick-up that will be in use in the cryogenic storage ring (CSR).

Kurzfassung

Schottkydiagnose am Schwerionen-Speicherring TSR

Bei der Schottkydiagnose wird das Rauschsignal eines Ionenstrahls in einem Speicherring untersucht, um Aussagen über Strahlcharakteristika wie die Impulsverteilung und die Strahlenergie zu machen. In der vorliegenden Arbeit wurde die Schottkydiagnose, sowie die Eigenschaften des Schottky Pick-ups theoretisch behandelt. In Experimenten mit zwei verschiedenen elektrostatischen Pick-ups konnten die Eigenschaften eines Schottky Pick-ups und die Theorie der Schottkydiagnose bestätigt werden. In den Experimenten wurde ein $^{12}C^{6+}$ Ionenstrahl mit einer Strahlenergie von 50 MeV verwendet. Vor der Analyse der Schottky-Rauschsignale musste berücksichtigt werden, dass das Signal vor der Messung durch Verstärker und das Durchlaufen langer Kabel verändert wird. Der Frequenzgang der verwendeten Kabel und Verstärker wurde daher gemessen und die Signale dementsprechend bereinigt. Nach Analyse der Daten wurden die Ergebnisse der Experimente mit den Erwartungen aus der Theorie verglichen. Schließlich wurden die Erkenntnisse dieser Arbeit verwendet, um einen Schottky Pick-up zu entwerfen, der in Zukunft im kryogenen Speicherring (CSR) verwendet wird.

Contents

1. Introduction

The Test Storage Ring (TSR) has been in operation at the Max Planck Institute for Nuclear Physics in Heidelberg since 1988 [1]. The TSR is an experimental facility for molecular, atomic and accelerator physics. With the installation of an electron cooler, the TSR has become the first heavy ion cooler ring. Figure 1.1 shows a sketch of the TSR, which is formed like a rounded square with two 45 ° dipole deflection magnets in each corner. Furthermore, two quadrupole doublets are located at each straight section and one quadrupole magnet in each corner to focus the beam. The straight sections between the quadrupoles have a length of 5.2 m, while the circumference of the whole ring is 55.42 m. Built into the straight sections are the septum for beam injection and extraction, the electron cooler, the electron target and a diagnostic section with a Schottky pick-up, an ion current monitor and an rf-resonator.
The electron cooler produces a cold electron beam at densities of up to 10^8 cm^{-3}. Under these conditions a decrease of phase space volume by a factor of $> 10^4$ has been achieved. Phase space compression of beams by electron cooling allows beams with an extremely small energy spread. The equilibrium values are determined by the balance of the frictional force of the cooling electrons and the heating by intra-beam scattering. One of the main research areas at the Max Planck Institute for Nuclear Physics (MPIK) is to study the interaction of molecular ions and highly charged atomic ions with electrons. For those experiments it is required to be able to determine the properties of the stored ion beam. Therefore, we depend on precise diagnostic methods to detect important beam parameters without influencing the beam itself. The momentum spread as well as the revolution frequency is easily extracted from the noise spectrum of the beam, the Schottky noise, which is related to its momentum distribution. In the following Bachelor thesis the characteristics of the Schottky harmonic spectrum, as well as the Schottky pick-up used to measure it, are to be determined and compared with theoretical calculations. Furthermore a conceptual design of the Schottky pick-up planned for the Cryogenic storage ring (CSR), which is currently under construction at the MPIK, will be given. The design will be based on the experimental results about the properties of a Schottky pick-up. Since

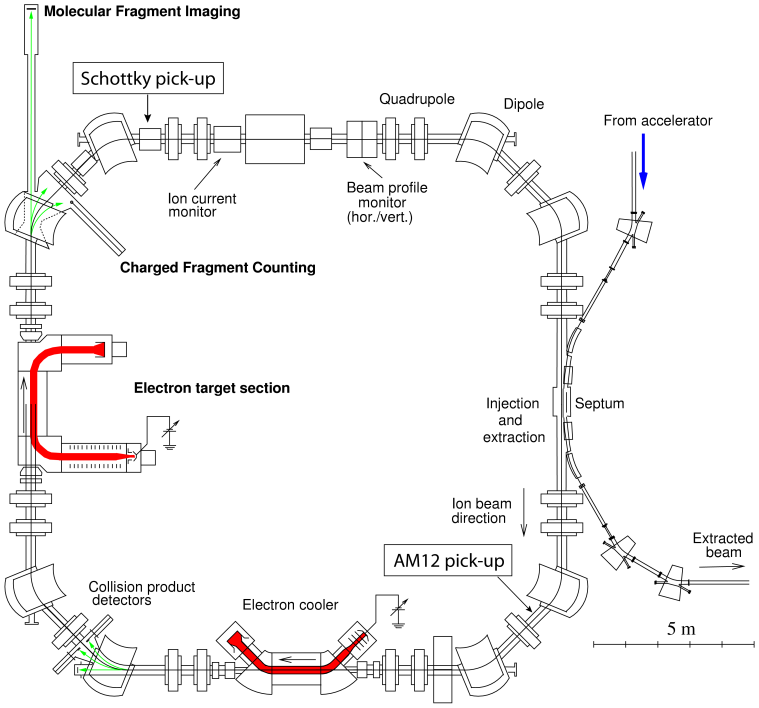

Figure 1.1: *The test storage ring with its most important elements. The TSR has a circumference of 55.42 m and the residual gas pressure is* $5 \cdot 10^{-11}$ *mbar*

Schottky diagnostics at the CSR will be carried out at very high harmonic numbers of the revolution frequency for slow ions, it is necessary to understand the characteristics of the whole harmonic spectrum.

2. The theory of Schottky noise diagnostics

2.1 Noise spectrum

To measure the revolution frequencey and momentum spread of a stored ion beam, Schottky noise diagnostics (see also [2]) is used, meaning that the noise spectrum of the ion beam current is measured. In order to calculate the noise spectrum, we first consider a single ion in the storage ring.

2.1.1 Noise signal of a single ion

The current $I(t)$ of a single ion with the charge Q at any given point in a storage ring can be described as a series of delta pulses (*see figure* 2.1). Between each of these lies an interval of $T = c_0/v$, where c_0 is the circumference of the ring and v is the velocity of the ion. This results in:

$$I_i(t) = Q \sum_n \delta(t - nT) \; . \tag{2.1}$$

The phase is arbitrarily set to 0 and varied later in equation (2.7).

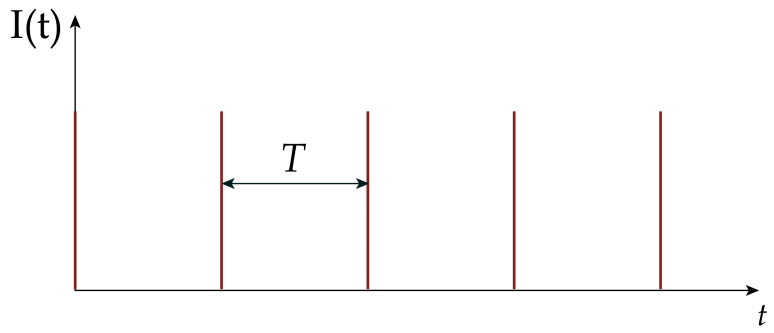

Figure 2.1: *Ion current of a single ion circulating in a storage ring*

Because this signal is a periodic function, it can be expressed as a Fourier series:

$$I_i(t) = \frac{a_0}{2} + \sum_{n=1}^{\infty}\Big(a_n \cos(n\frac{2\pi}{T}t) + b_n \sin(n\frac{2\pi}{T}t)\Big) , \tag{2.2}$$

with

$$\omega_0 = \frac{2\pi}{T} \tag{2.3}$$

$$a_n = \frac{2}{T}\int_{-T/2}^{T/2} Q\,\delta(t-nT)\cos(n\frac{2\pi}{T}t)\mathrm{d}t = \frac{2Q}{T} \tag{2.4}$$

$$b_n = \frac{2}{T}\int_{-T/2}^{T/2} Q\,\delta(t-nT)\sin(n\frac{2\pi}{T}t)\mathrm{d}t = 0 , \tag{2.5}$$

which yields:

$$I_i(t) = \frac{Q}{T} + \sum_{n=1}^{\infty}\frac{2Q}{T}\cos(n\omega_0 t) . \tag{2.6}$$

Figure 2.2 shows the related spectrum $\hat{I}_n$ of the ion in the storage ring. The spectrum is a series of delta pulses at multiples, called harmonics, of the revolution frequency f_0, with $f_0 = \omega_0/2\pi = 1/T$.

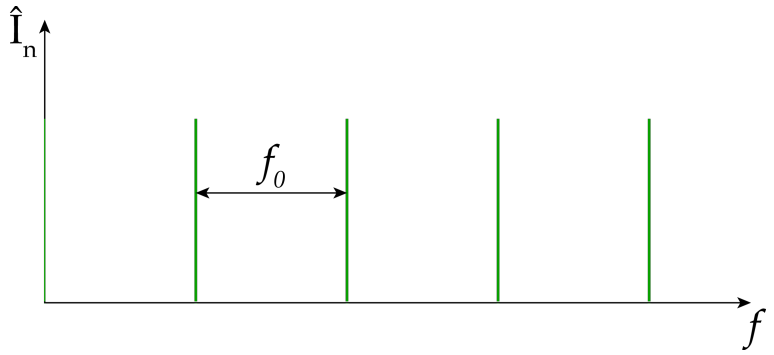

Figure 2.2: *Spectrum of the ion current of a single ion circulating in a storage ring*

2.1.2 Noise signal of N monoenergetic ions

The stored ion current of an ion beam that consists of N monoenergetic ions with the charge Q can be expressed by:

$$I(t) = \sum_{i=1}^{N}\Big(\frac{Q}{T} + \sum_{n=1}^{\infty}\frac{2Q}{T}\cos(n(\omega_0 t - \varphi_i))\Big) \tag{2.7}$$

$$= \frac{NQ}{T} + \sum_{n=1}^{\infty}\sum_{i=1}^{N}\frac{2Q}{T}\cos(n(\omega_0 t - \varphi_i)) \tag{2.8}$$

$$= \frac{NQ}{T} + \sum_{n=1}^{\infty}\sum_{i=1}^{N}\frac{2Q}{T}\cos\Big((n\omega_0 t)\cos(n\varphi_i) - \sin(n\omega_0 t)\sin(n\varphi_i)\Big)\,, \tag{2.9}$$

with the random phase φ_i, which depends on the time at which the ion arrives at the given point in the storage ring. This current can also be written as

$$I(t) = \frac{NQ}{T} + \sum_{n=1}^{\infty}\Big(A_n\cos(n\omega_0 t) - B_n\sin(n\omega_0 t)\Big)\,, \tag{2.10}$$

with

$$A_n = \sum_{i=1}^{N}\frac{2Q}{T}\cos(n\varphi_i) \qquad B_n = -\sum_{i=1}^{N}\frac{2Q}{T}\sin(n\varphi_i)\,. \tag{2.11}$$

To determine the spectral lines we need

$$A_n^2 = \Big(\frac{2Q}{T}\Big)^2\Big(\sum_{i=1}^{N}\cos(n\varphi_i)\Big)^2 \qquad \text{and} \tag{2.12}$$

$$B_n^2 = \Big(\frac{2Q}{T}\Big)^2\Big(\sum_{i=1}^{N}\sin(n\varphi_i)\Big)^2 \tag{2.13}$$

Because the phases φ_i are randomly distributed, for a large number of ions N, we obtain:

$$\sum_{i\neq j}^{N}\cos\varphi_i\cos\varphi_j = 0 \qquad \text{and} \qquad \sum_{i=1}^{N}\cos^2\varphi_i = \frac{N}{2}\,, \tag{2.14}$$

and similarly:

$$\sum_{i\neq j}^{N}\sin\varphi_i\sin\varphi_j = 0 \qquad \text{and} \qquad \sum_{i=1}^{N}\sin^2\varphi_i = \frac{N}{2}\,, \tag{2.15}$$

which yields:

$$A_n^2 = \Big(\frac{2Q}{T}\Big)^2\frac{N}{2} = 2N\Big(\frac{Q}{T}\Big)^2 \qquad \text{and} \tag{2.16}$$

$$B_n^2 = 2N\Big(\frac{Q}{T}\Big)^2\,. \tag{2.17}$$

From this, we can conclude that the spectral lines of a monoenergetic beam are:

$$\hat{I}_n = \sqrt{A_n^2 + B_n^2} \tag{2.18}$$

$$= \frac{2Q}{T}\sqrt{N} \tag{2.19}$$

at frequencies $n \cdot \omega_0$. The spectral power is correspondingly:

$$\hat{I}_n^2 = \left(\frac{2Q}{T}\right)^2 N\,. \tag{2.20}$$

2.1.3 Noise signal of an ion beam

If we observe the spectrum of a single ion with the revolution frequency $f_{0,1}$, we get a series of delta pulses. A second ion with a different frequency $f_{0,2}$ renders a series of delta pulses that are shifted from those of the first ion.

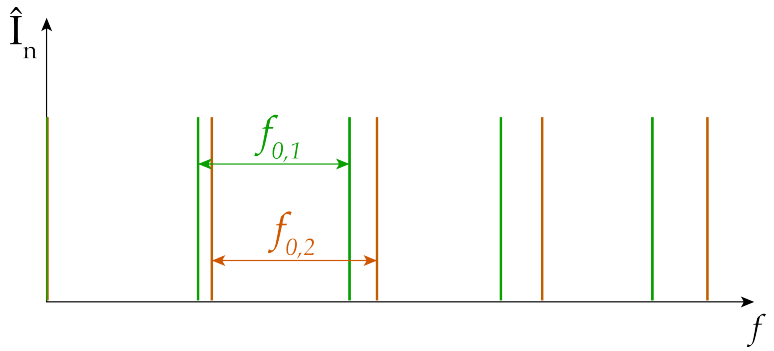

Figure 2.3: *Spectrum of two ions with different revolution frequencies $f_{0,1}$ and $f_{0,2}$*

The spectral distance between the delta pulses from the two different ions is given by $(f_{0,1} - f_{0,2})\,n$. This means that the higher the harmonic number, the further apart the two pulses are. How far apart they are is also dependent on the difference between the revolution frequencies and therefore dependent on the difference in velocity (or momentum) of the ions. For many ions, the delta pulses form a Schottky band with a certain height and width, the width of which is connected to the momentum spread of the ions.

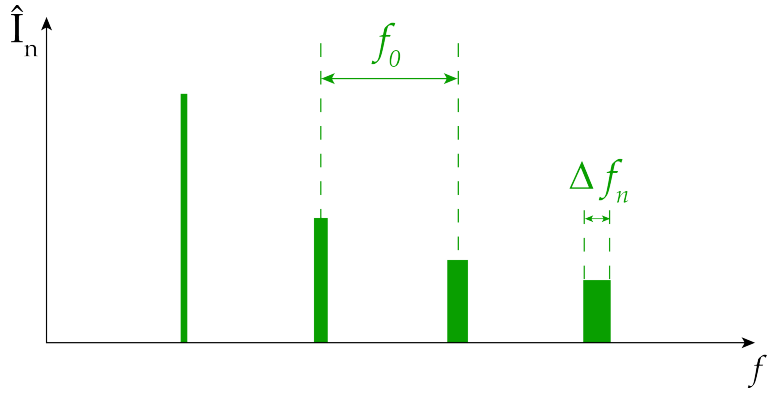

Figure 2.4: *Spectrum of an ion beam. Schottky bands form at harmonics of the average revolution frequency* f_0

The width of the nth Schottky band is given by $\Delta f_n = n\Delta f_0$, where Δf_0 depends on the momentum spread Δp of the ion beam:

$$\frac{f_0}{\Delta f_0} = \frac{1}{\eta}\frac{p}{\Delta p} . \tag{2.21}$$

η is the slip factor of the storage ring and describes the dependency of the average revolution frequency f_0 on the ion momentum p. In the standard mode of the TSR, $\eta = 0.89$. The revolution frequencies of an ion beam with an energy spread can be described by a distribution function $D(f_0) = \mathrm{d}N/\mathrm{d}f_0$. Therefore, the spectral power changes into a spectral power density:

$$\frac{\mathrm{d}\hat{I}_n^2}{\mathrm{d}f} = \left(\frac{2Q}{T}\right)^2 \frac{\mathrm{d}N}{\mathrm{d}f} = \left(\frac{2Q}{T}\right)^2 D(f_0) \quad \text{with} \quad f = n \cdot f_0 . \tag{2.22}$$

The power of each Schottky band remains constant:

$$\int \frac{\mathrm{d}\hat{I}_n^2}{\mathrm{d}f_0}\,\mathrm{d}f = \left(\frac{2Q}{T}\right)^2 N . \tag{2.23}$$

2.2 Measured spectrum

2.2.1 Signal of a single ion

To detect the ion beam without influencing the beam itself a Schottky pick-up is used. Figure 2.5 shows a sketch of a simple Schottky pick-up, which is a conductive tube around the ion beam. In the diagram, C describes the capacity of the pick-up and the cable that connects the pick-up with a preamplifier plus the input capacity of the preamplifier itself. R describes the input resistance of the preamplifier.

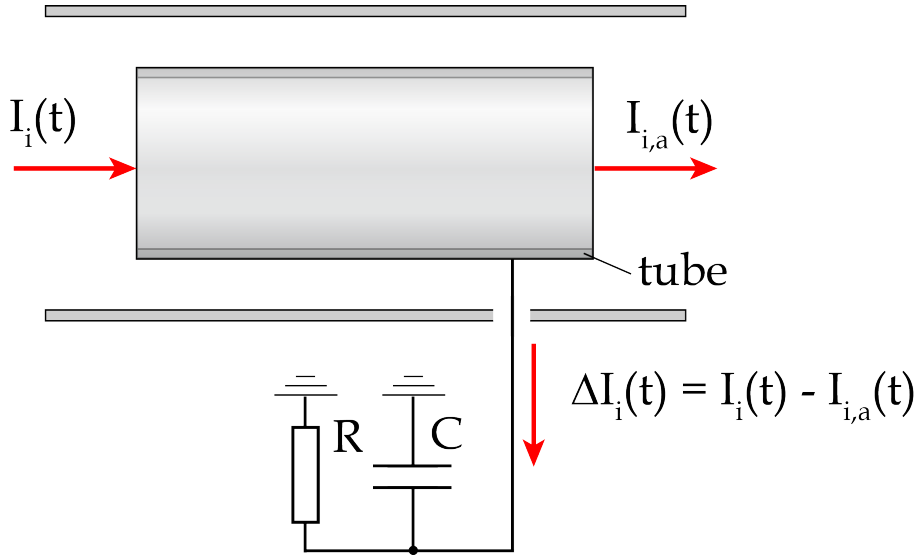

Figure 2.5: *Sketch of a Schottky pick-up including its capacitance C and the resistance R from the preamplifier that is used to increase the signal.*

The current of a single ion moving through a storage ring at the entrance of the tube can be described by:

$$I_i(t) = Q \sum_n \delta(t - nT) \ . \tag{2.24}$$

Whereas the current at the exit of the tube is given by

$$I_{i,a}(t) = I_i(t - \Delta t) = Q \sum_n \delta(t - nT + \Delta t) \ , \tag{2.25}$$

where Δt is the flight time through the pick-up:

$$\Delta t = \frac{L}{v} \ , \tag{2.26}$$

with L being the length of the pick-up and v the velocity of the ions.

As with any periodic signal, the currents can be expressed in a Fourier series (*see also* (2.2)). For the current entering the pick-up we obtain:

$$I_i(t) \quad = \quad \frac{a_0}{2} + \sum_{n=1}^{\infty} \Big(a_n \cos(n \frac{2\pi}{T} t) + b_n \sin(n \frac{2\pi}{T} t) \Big) \ , \tag{2.27}$$

with the Fourier coefficients

$$a_n = \frac{2}{T}\int_{-T/2}^{T/2} Q\delta(t-nT)\cos(n\frac{2\pi}{T}t)\mathrm{d}t = \frac{2Q}{T} \tag{2.28}$$

$$b_n = \frac{2}{T}\int_{-T/2}^{T/2} Q\delta(t-nT)\sin(n\frac{2\pi}{T}t)\mathrm{d}t = 0\,. \tag{2.29}$$

at frequencies $\omega_0 = 2\pi/T$, which yields

$$I_i(t) = \frac{Q}{T} + \sum_{n=1}^{\infty}\frac{2Q}{T}\cos(n\omega_0 t)\,. \tag{2.30}$$

The Fourier series of the current leaving the pick-up is given by

$$I_{i,a}(t) = \frac{a_0}{2} + \sum_{n=1}^{\infty}\Big(a_n\cos(n\frac{2\pi}{T}t) + b_n\sin(n\frac{2\pi}{T}t)\Big) \tag{2.31}$$

with the Fourier coefficients

$$a_n = \frac{2}{T}\int_{-T/2}^{T/2} Q\delta(t-nT+\Delta t)\cos(n\frac{2\pi}{T}t)\mathrm{d}t = \frac{2Q}{T}\cos(n\omega_0\frac{L}{v}) \tag{2.32}$$

$$b_n = \frac{2}{T}\int_{-T/2}^{T/2} Q\delta(t-nT+\Delta t)\sin(n\frac{2\pi}{T}t)\mathrm{d}t = -\frac{2Q}{T}\sin(n\omega_0\frac{L}{v})\,, \tag{2.33}$$

which yields:

$$I_{i,a}(t) = \frac{Q}{T} + \sum_{n=1}^{\infty}\Big(\frac{2Q}{T}\cos(n\omega_0\frac{L}{v})\cos(n\omega_0 t) - \frac{2Q}{T}\sin(n\omega_0\frac{L}{v})\sin(n\omega_0 t)\Big)\,. \tag{2.34}$$

The current that flows into the measuring RC circuit is given by $\Delta I_i(t) = I_i(t) - I_{i,a}(t)$, the difference between the exit and the entrance current:

$$\Delta I_i(t) = \frac{2Q}{T}\sum_{n=1}^{\infty}\Big((1-\cos(\omega_n\frac{L}{v}))\cos(\omega_n t) - \sin(\omega_n\frac{L}{v})\sin(\omega_n t)\Big)\,. \tag{2.35}$$

If we look at the amplitude $\Delta\hat{I}_i$ of the current at the frequencies ω_n, we can see that the spectrum of the current that flows into the circuit from a single ion is:

$$\Delta\hat{I}_i(\omega_n) = \frac{2Q}{T}\sqrt{\Big(1-\cos(\omega_n\frac{L}{v})\Big)^2 + \sin^2(\omega_n\frac{L}{v})} \tag{2.36}$$

$$= \frac{2\sqrt{2}Q}{T}\sqrt{1-\cos(\omega_n\frac{L}{v})}\,. \tag{2.37}$$

As seen in figure 2.5, the Schottky pick-up can be described as a capacity C with a parallel resistance R from the input resistance of the preamplifier. The impedance Z of the system is:

$$\frac{1}{Z} = \frac{1}{R} + i\omega_n C \ . \tag{2.38}$$

Therefore the voltage induced by one single ion is given by

$$\hat{U}_i(\omega_n) = |Z|\Delta\hat{I}_i(\omega_n) = \frac{R}{\sqrt{1+\omega_n^2 C^2 R^2}} \frac{2\sqrt{2}Q}{T} \sqrt{1-\cos(\omega_n \frac{L}{v})} \ . \tag{2.39}$$

2.2.2 Signal of the ion beam

Now we consider the signal of N Ions with the charge Q interacting with the tube. The induced voltage in the measurement circuit is the same for every ion, however, each ion has a different phase (*see also equation* (2.7)).

$$\hat{U}(\omega_n) = \sum_{i=1}^{N} \hat{U}_i(\omega_n) \cos\varphi_i \tag{2.40}$$

Because the phases φ_i are randomly distributed, the signal $\hat{U}(\omega_n)$ of the whole beam averages to zero over time. Therefore we observe the Schottky power, which is defined as:

$$P_0(\omega_n) \quad = \quad \Big(\sum_{i=1}^{N} \hat{U}_i(\omega_n) \cos\varphi_i\Big)^2 \tag{2.41}$$

As was shown in equation (2.14), for randomly distributed phases φ_i and a large number of ions N, we obtain:

$$\Big(\sum_{i=1}^{N} \cos\varphi_i\Big)^2 = \frac{N}{2} \tag{2.42}$$

$\hat{U}_i(\omega_n)$ is equal for all ions, so the Schottky power at harmonic numbers n is given by

$$P_0(\omega_n) \quad = \quad \frac{N}{2}\hat{U}_i^2(\omega_n) \tag{2.43}$$

$$\quad = \quad \frac{4NQ^2}{T^2} \frac{R^2}{1+\omega_n^2 C^2 R^2} \Big(1-\cos(\omega_n \frac{L}{v})\Big) \ . \tag{2.44}$$

2.3 Expected results and applied pick-up geometries

The Schottky pick-up that is currently used in the TSR is not a closed tube as we previously assumed in our calculations. The existing Schottky pick-up is made up of four 4

cm wide conduction strip lines, each located at about 8 cm from the center of the beam path in opposing corners.

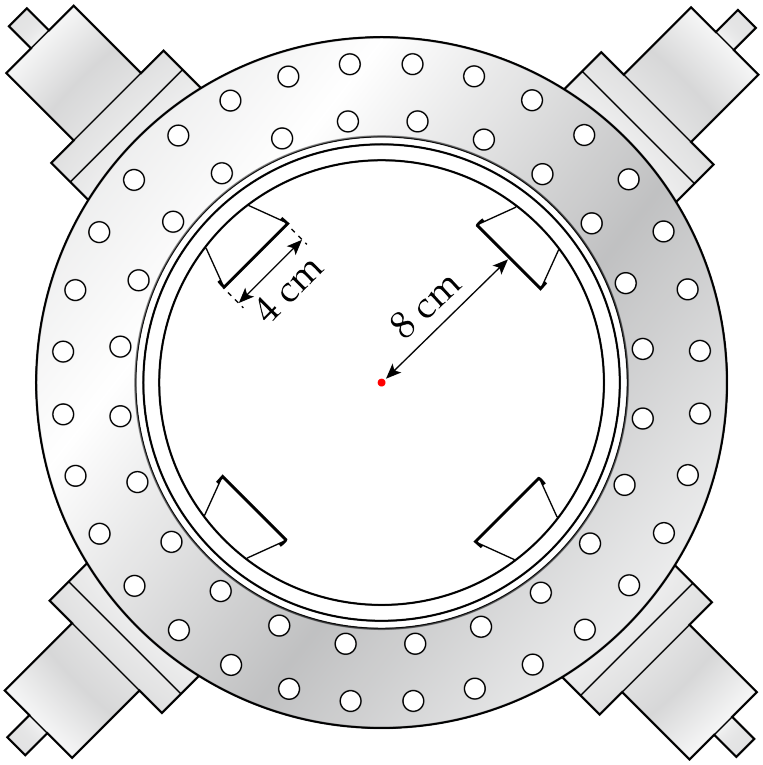

Figure 2.6: *Sketch of the Schottky pick-up of the TSR*

Because of this arrangement we can treat the voltage signal that is induced on one strip line of the pick-up as proportional to one that we would get if we had a closed tube, with a scaling factor κ, where κ is the ratio between the width of one strip line and the circumference of a tube with a radius which corresponds to the distance of one strip line to the beam center:

$$\kappa = \frac{\text{width of one strip line}}{\text{circumference of tube}} \, . \tag{2.45}$$

Because the power is proportional to the square of the voltage $P \sim U^2$, the power we measure with one strip line of our pick-up is proportional to κ^2:

$$P(\omega_n) = \kappa^2 \, P_0(\omega_n) \, . \tag{2.46}$$

The Schottky pick-up currently in use at the TSR has the following properties

$$\text{Length } L = 46.2 \text{ cm} \quad \text{Capacity } C = 68 \text{ pF}$$

A $^{12}C^{6+}$ beam with the energy $E = 50.4$ MeV, as used in the experiment, has a revolution frequency of about $f_0 = \omega_0/2\pi = 512$ kHz. The circumference of the TSR is $c_0 = 55.42$ m.

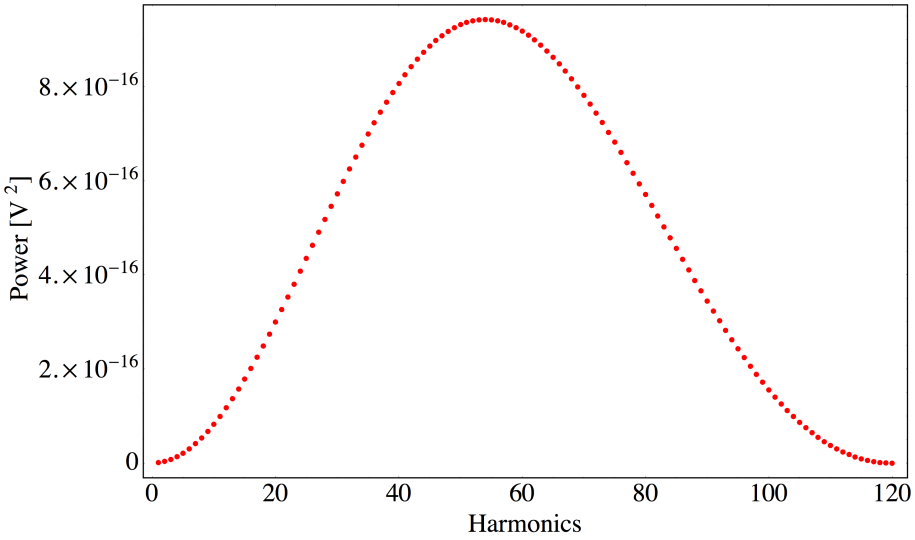

Figure 2.7: *Expected Schottky power harmonic spectrum for a 50 MeV $^{12}C^{6+}$ ion beam using a preamplifier with 50 Ω input resistance on one strip line of the Schottky pick-up.*

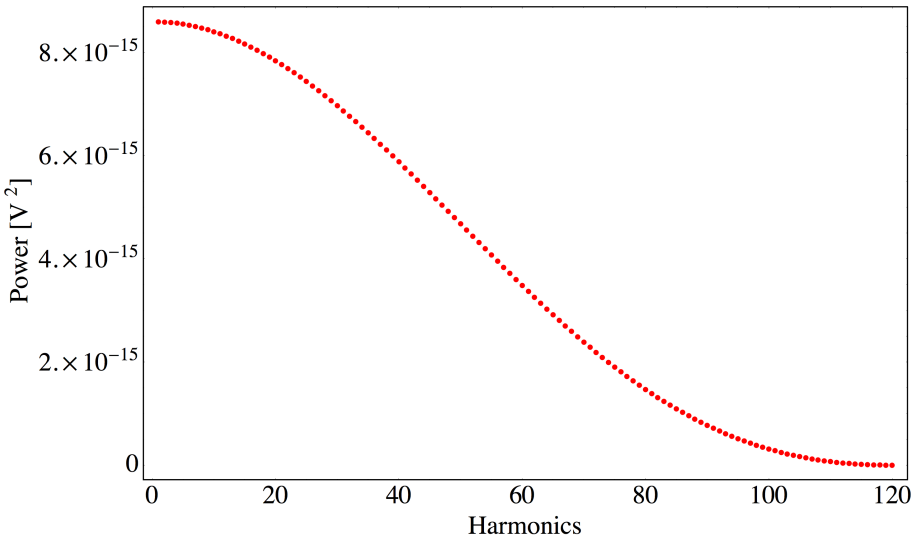

Figure 2.8: *Expected Schottky power harmonic spectrum for a 50 MeV $^{12}C^{6+}$ ion beam using a preamplifier with 1 MΩ input resistance and an additional capacitance of 50 pF on one strip line of the Schottky pick-up.*

The experiment was conducted with an ion current of $I = 20$ μA and a preamplifier with an input resistance of $R = 50$ Ω. The expected result for the measured power at different

harmonic numbers n is:

$$P(n) = \kappa^2 \frac{4}{T} \frac{IQR^2}{1 + n^2\omega_o^2 C^2 R^2} \left(1 - \cos(n2\pi \frac{L}{c_0})\right) . \tag{2.47}$$

If the experiment is carried out with a preamplifier with an input resistance of 1 MΩ, the signal at lower frequencies is not surpressed (*see figure* 2.8).

Another pick-up that is used in the measurements is the AM12 position pick-up. It is a diagnostic tool in the TSR that allows us to determine the position of the stored ion beam. It consists of two parts, the horizontal pick-up, to determine the horizontal beam position and the vertical pick-up to determine the vertical beam position (*see figure* 2.9). For the measurement, only the vertical pick-up was used, which is a tube of 8.6 cm length and 10 cm radius with a slit that divides it diagonally to measure the location of the beam. Its capacitance, including the cables which connect it to the amplifier, is C = 176 pF. Using it as a pick-up to measure the Schottky harmonic spectrum, both parts of the vertical pick-up were connected. As the vertical pick up is a closed tube, except for the negligible diagonal slit, the theoretical value for κ is 1.

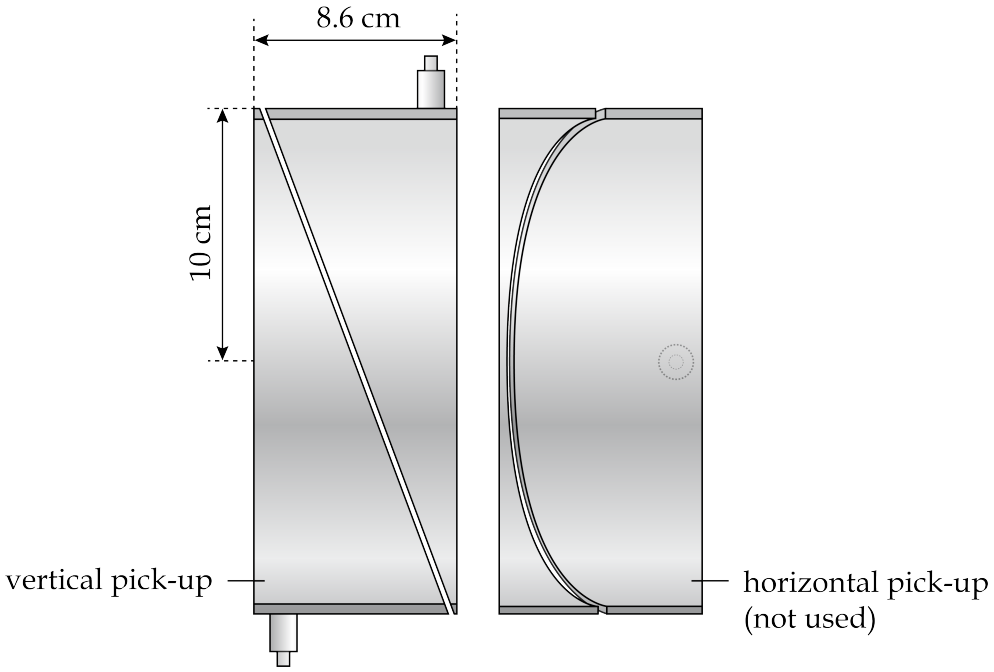

Figure 2.9: *Sketch of the AM12 position pick-up in side view. Only the vertical pick-up was used in the measurements.*

2.4 Determining the beam parameters

For precision experiments in molecular and atomic physics at the TSR it is extremely important to determine the properties of the ion beam, most of all the energy and the momentum spread. To determine those parameters, we measure the width of the Schottky band Δf_n and the center frequency f_n at a certain harmonic n.
From the frequency f_n we are able to determine the revolution frequency and from that the velocity of the beam:

$$f_0 = \frac{f_n}{n} \qquad v = f_0 \cdot c_0 \ ,$$

with the circumference of the ring, c_0. The kinetic energy of ions with the mass m is given by

$$E = (\gamma - 1)\, mc^2 \qquad \text{with} \qquad \gamma = \frac{1}{\sqrt{1 - (\frac{v}{c})^2}} \ . \tag{2.48}$$

The momentum spread can be determined by:

$$\Delta p = \frac{1}{\eta}\, \frac{p}{f_n}\, \Delta f_n \qquad \text{with} \qquad p = mv \ , \tag{2.49}$$

where $\eta = 0.89$ in the standard mode of the TSR.

3. Measurement of the Schottky harmonic spectrum

In this chapter the measurements of Schottky harmonic spectra performed with different experimental setups are presented and compared to the theory of Schottky diagnostics. The measurements were made with two electrostatic pick-ups of different length and design, using a $^{12}C^{6+}$ ion beam with an energy of 50 MeV. The signals from the pick-ups are amplified using one of three different amplifiers. The preamplifiers that are used are shown in the table below, with their input resistance R and input capacity C. The short name is the name by which the amplifiers will be referred to when describing the measurements.

Amplifier	Short name	R [Ω]	Frequency range	Gain [dB]	C [pF]
Miteq	Miteq	50	1 - 100 MHz	46	~ 0
NF SA-230F5	NF 50 Ω	50	100 kHz - 100 MHz	44	~ 0
NF SA-220F5	NF 1 MΩ	10^6	400 Hz - 140 MHz	40	~ 50

The NF 1 MΩ amplifier needed to be repaired before, so the actual values for the input resistance and capacitance might vary from those provided by the manufacturer. Four identical Miteq amplifiers are available for measurements with all four strip lines of the Schottky pick-up.

3.1 The experimental setup

After being amplified the signal is conveyed to the control desk by an approximately 100 m long double screened cable. At the control desk a Tektronix RSA 3303A spectrum analyzer is used to record the spectrum of the signal.

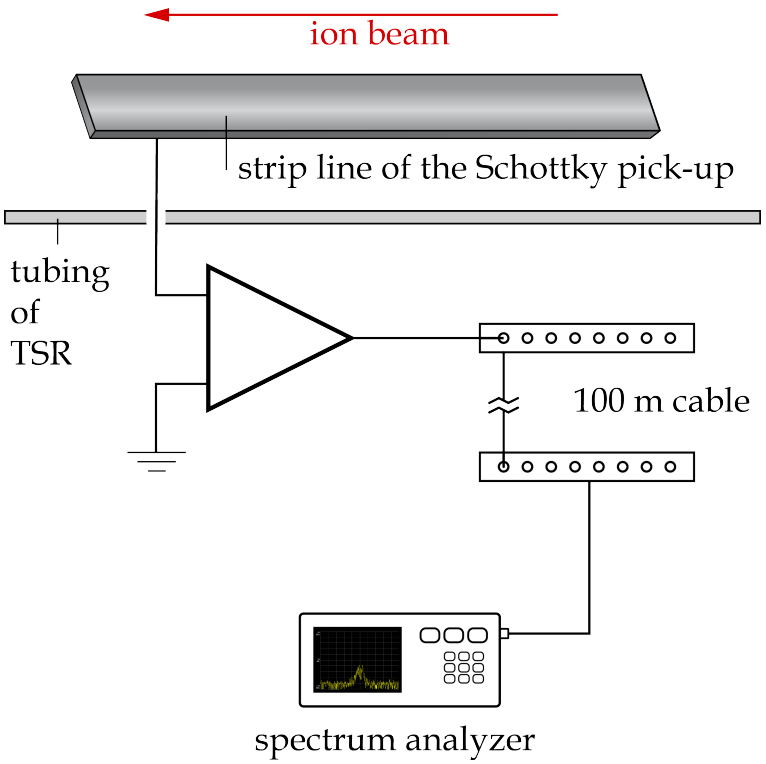

Figure 3.1: *Experimental setup for the measurement of the harmonic spectrum. The signals from the Schottky pick-up are amplified and sent back to the control desk to be measured by a spectrum analyzer.*

In this setup, the frequency response of the signal is mainly altered by the amplifier and by the 100 m long cable between the amplifier output and the control desk. To be able to compare the signal to the theoretical values we must first correct the signal based on the frequency response of both the cable and the amplifier.

3.1.1 Damping of the signal

The damping of an rf-signal flowing through a cable can largely be described by two processes, resistive losses and losses in the dielectric. A cable can be represented by the schematic diagram seen in figure 3.2.
The resistance R', with $R'= R/\text{length}$, can be derived from the skin effect. An alternating current flowing through a cylindrical conductor causes eddy currents that produce a countervoltage inside the conductor, which leads to the current being pushed to the skin of the conductor, thereby reducing the conducting cross section. Therefore, the resistance of a cable to an alternating current is equal to the resistance of a hollow tube with wall thickness δ (also called skin depth) to a direct current. The resistance to a current is

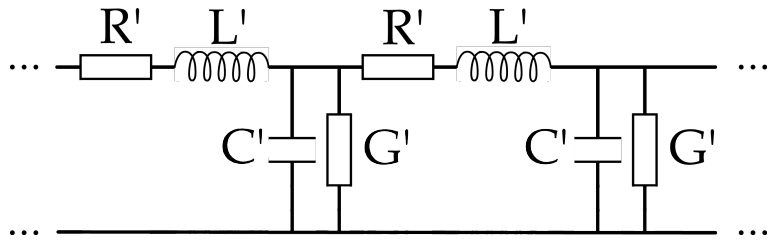

Figure 3.2: *Schematic diagram of a cable, with capacity per unit length C', inductivity per unit length L', resistance per unit length R' and leakage conductance per unit length G'.*

given by

$$R' = \frac{\rho}{A} \,, \tag{3.1}$$

where ρ is the resistivity of the conductor and A is the area of the cross section. The cross sectional area in this case is given by

$$A = (D - \delta)\delta\pi \approx D\delta\pi \tag{3.2}$$

where δ is the thickness of the conducting layer caused by the skin effect and D is the diameter of the cable.

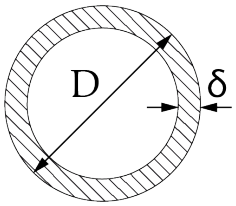

Figure 3.3: *Schematical cross section of a cable with diameter D and skin depth δ.*

The skin depth δ is given by [3]

$$\delta = \frac{1}{\sqrt{\pi\mu\sigma}} \frac{1}{\sqrt{f}} \tag{3.3}$$

where μ is the permeability and σ the electrical conductivity of the material and f is the frequency of the signal flowing through the cable. The resistance of the cable induced by the skin effect can thus be expressed by:

$$R' = \frac{\rho}{D\pi}\sqrt{\pi\mu\sigma}\,\sqrt{f} \;\sim \sqrt{f} \tag{3.4}$$

The leakage conductance G' describes the losses in the dielectric due to the quick changes of the electric field. G' is proportional to the frequency f of the current flowing through the cable [4]:

$$G' \sim f \ . \tag{3.5}$$

The voltage U along the cable can be described by the wave equation

$$\frac{\mathrm{d}^2 U(z)}{\mathrm{d}z^2} = \gamma^2 \, U(z) \ , \tag{3.6}$$

with z being the position along the cable and

$$\gamma = \sqrt{(R' + i\omega L')(G' + i\omega C')} = \alpha + i\beta \ , \tag{3.7}$$

where α is the damping coefficient and β is a phase coefficient [4].
The general solution for this equation is:

$$U = U_0 e^{-\gamma z} + U_1 e^{\gamma z} \ . \tag{3.8}$$

As the cable is closed with its characteristic wave impedance of 50 Ω, there is no reflection inside the cable, so only the signal in one direction remains:

$$U = U_0 e^{-\gamma z} \ . \tag{3.9}$$

Therefore the ratio of the voltage U after a certain length to the initial voltage U_0 can be described by:

$$\ln \left| \frac{U}{U_0} \right| = -\alpha \cdot z \ , \tag{3.10}$$

where α is given by [4]

$$\alpha = \frac{R'}{2} \sqrt{\frac{C'}{L'}} + \frac{G'}{2} \sqrt{\frac{L'}{C'}} \tag{3.11}$$

at high frequencies.
Using equation (3.10), the damping x_D of a cable with the length z is given by

$$x_D = 20 \log \left| \frac{U}{U_0} \right| = -20 \log(e) \cdot \alpha \cdot z \ \sim \ \alpha \ . \tag{3.12}$$

Therefore the fit function that was used to characterize the measured damping of a cable is:

$$x_D = C_1 f + C_2 \sqrt{f} \ , \tag{3.13}$$

with the fit parameters C_1 and C_2.

Ten new double shielded cables of about 100 m length were installed between the TSR and the control desk (cables No. 1 to No. 10). To determine the damping of the cables a Hewlett Packard 4396A network analyzer was used. The cables are identical and should therefore have the same damping. Nevertheless, the damping of each one was determined to confirm this.

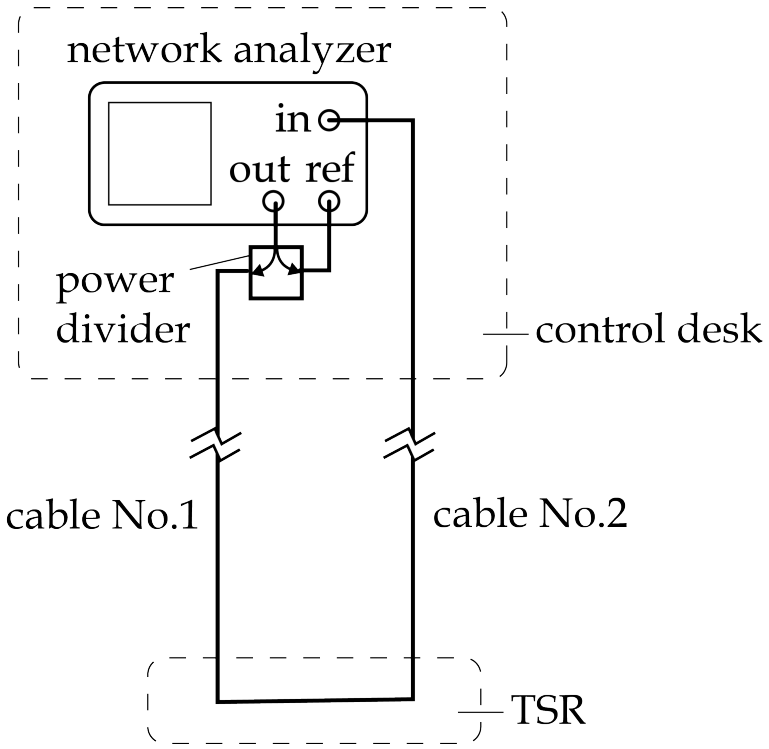

Figure 3.4: *Experimental setup to measure the damping of the cables between the TSR and the control desk.*

First, the damping of cables No. 1 - No. 3 was determined. To do this, an alternating voltage from the output of the network analyzer was applied to cable No. 1. At the other end the cable was directly connected to cable No. 2 and the voltage was sent back to the input of the network analyzer via cable No. 2 (*see figure* 3.4).

The frequency response of this setup was recorded and afterwards repeated with cables No. 1 and 3 and No. 2 and 3, resulting in three equations for the damping, where $x_{D,ij}$

describes the total damping of cables i and j:

$$x_{D,12}(f) = x_{D,1}(f) + x_{D,2}(f) \tag{3.14}$$
$$x_{D,13}(f) = x_{D,1}(f) + x_{D,3}(f) \tag{3.15}$$
$$x_{D,23}(f) = x_{D,2}(f) + x_{D,3}(f) \tag{3.16}$$

This allows us to calculate the damping of each of the three cables $x_{D,1}(f)$, $x_{D,2}(f)$, $x_{D,3}(f)$ from the measurement of $x_{D,12}(f)$, $x_{D,13}(f)$, $x_{D,23}(f)$ (*see figure* 3.5) by solving the equation system (3.14) - (3.16). Afterwards, cables No. 4 - No. 10 were measured together with cable No. 1 to determine their damping:

$$x_{D,i}(f) = x_{D,i1}(f) - x_{D,1}(f) \tag{3.17}$$

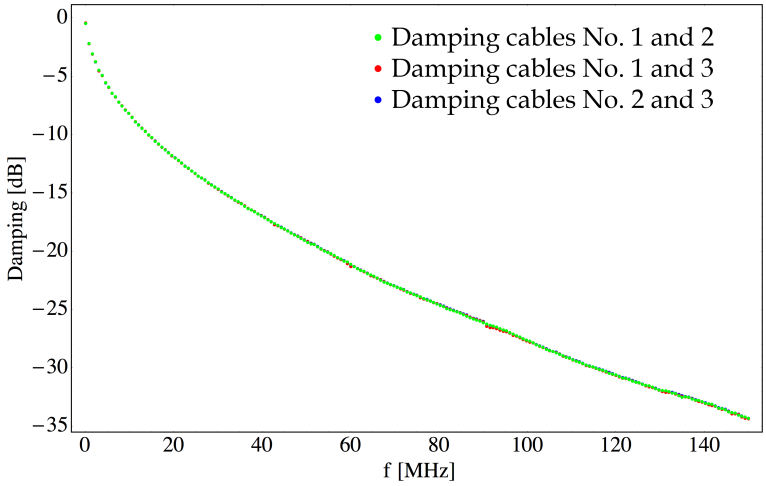

Figure 3.5: *Measurement of the damping of cables No. 1 and 2, $x_{D,12}(f)$, cables No. 1 and 3, $x_{D,13}(f)$ and cables No. 2 and 3, $x_{D,23}(f)$.*

The equation system (3.14) - (3.16) and equation (3.17) was solved for each frequency measuring point, the damping for each cable is shown in figure 3.6.

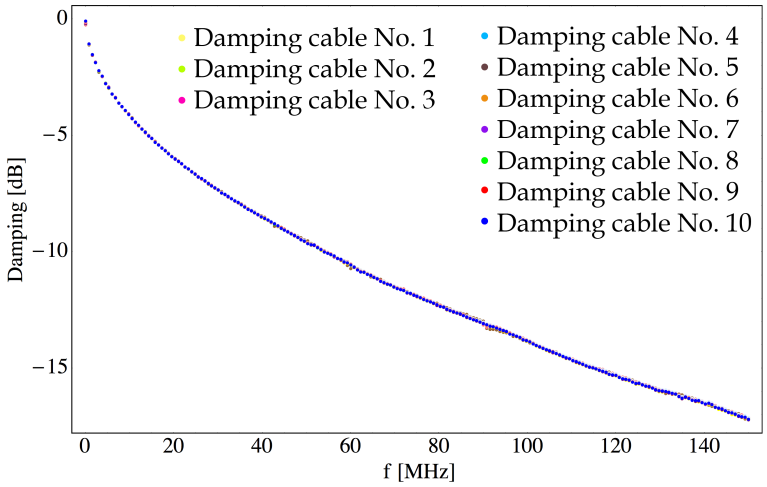

Figure 3.6: *Damping of the 100 m double screened cables No. 1 to No. 10.*

It is evident that the cables all have the same damping. Using the fit function from equation 3.13 to find a fit for the measuring points results in:

$$x_D(f) \;=\; -\,0.0093\,f - 1.290\,\sqrt{f} \tag{3.18}$$

Where f is the frequency in MHz. The result is shown in figure 3.7.

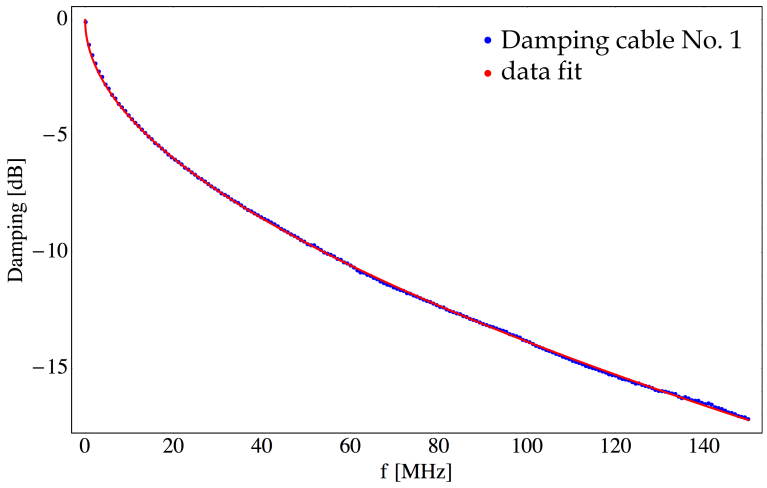

Figure 3.7: *Damping of cable No. 10 and the fit through the data points.*

3.1.2 Frequency response of the amplifiers

Another component that alters the signal is the amplifier used in the setup. The frequency response of the amplifiers is detected using the same network analyzer that registered the

damping of the cables. To prevent reflections along the cables, a 50 Ω resistance was added parallel to the input resistance of the NF 1 MΩ amplifier, while measuring its frequency response.

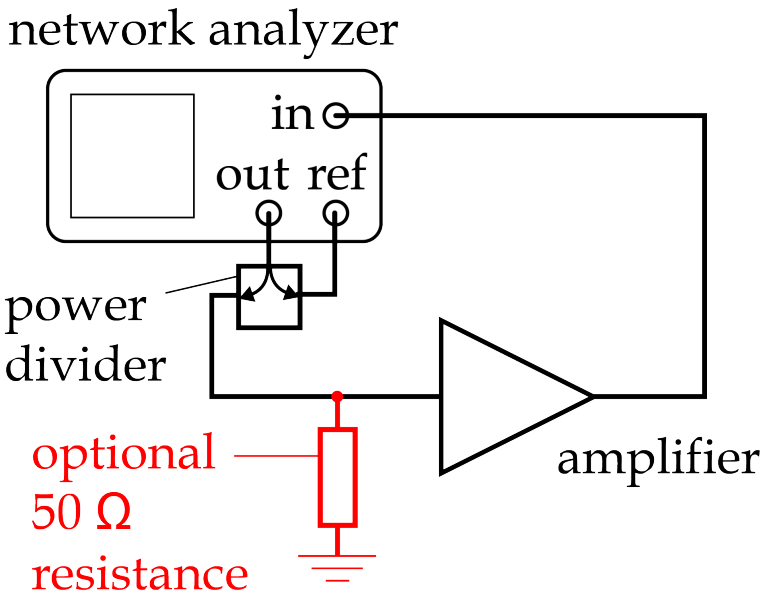

Figure 3.8: *Setup to measure the frequency response of the amplifiers. For the NF 1 MΩ amplifier a resistance is added to avoid reflections.*

A polynomial function was used to fit the data. Figure 3.9 shows the frequency response of one of the amplifiers, the NF 50 Ω, as an example.

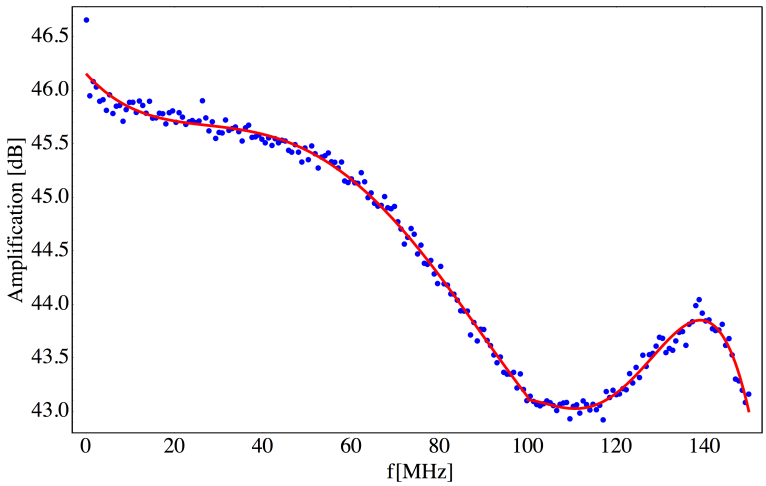

Figure 3.9: *The measured frequency response of the NF 50 Ω amplifier and the fit through the data points, using a piecewise polynomial function.*

3.2 The measurement

The spectrum analyzer Tektronix RSA 3303A was used to measure the Schottky harmonic spectra. For this, the power of the Schottky band at each harmonic number was measured. The power that is being recorded is measured across a certain resolution bandwidth, which must be taken into account when analyzing the data. To obtain a spectral power density, the power is divided by the resolution bandwidth. Figure 3.10 shows the power signal of the Schottky band at the 60^{th} harmonic of the revolution frequency, measured with the spectrum analyzer in the setup shown in figure 3.1, using a 50 MeV $^{12}C^{6+}$ ion beam (I = 20 μA) and using one strip line of the Schottky pick-up. The spectrum that is shown has not been corrected for the amplification and the damping of the cables.

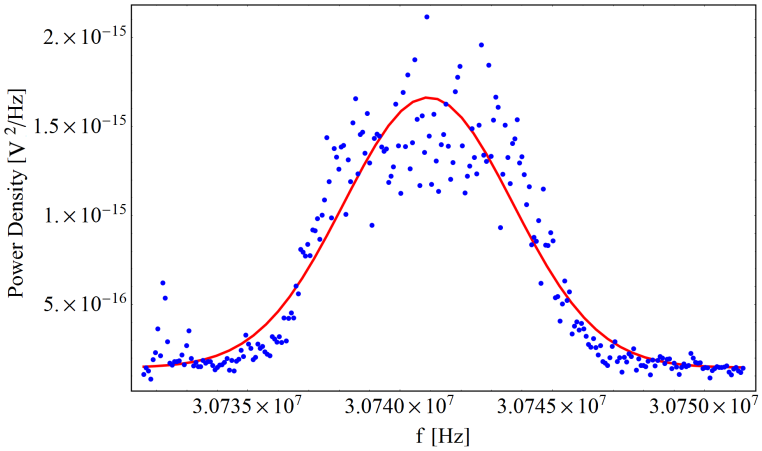

Figure 3.10: *The spectral power density of the Schottky band at the 60^{th} harmonic, measured with one strip line of the Schottky pick-up, the NF 50 Ω amplifier and an ion current of I = 20 μA, not yet corrected for amplification and damping.*

A Gaussian function was used to fit the data:

$$P'(f) = \frac{A}{\sqrt{2\pi}\sigma} \exp\left(-\frac{(f-f_0)^2}{2\sigma^2}\right) + B \tag{3.19}$$

The fit parameter A describes the integral over the Gaussian function and represents the total power of one Schottky band. The power from each Schottky band is recorded and afterwards corrected using the frequency response function from the damping of the cable and the amplifier. The corrected power of each Schottky band at the different harmonics is then plotted against the harmonic number n (*see figure* 3.11), resulting in the harmonic spectrum.

3.2.1 Measurement with the Schottky pick-up

The Schottky harmonic spectrum measured with one strip line of the Schottky pick-up and the NF 50 Ω amplifier is shown in figure 3.11. It shows the power in each Schottky band as a function of the harmonic number of the revolution frequency $f_0 = 512$ kHz for a 50 MeV $^{12}C^{6+}$ ion beam with a current of I = 20 μA.

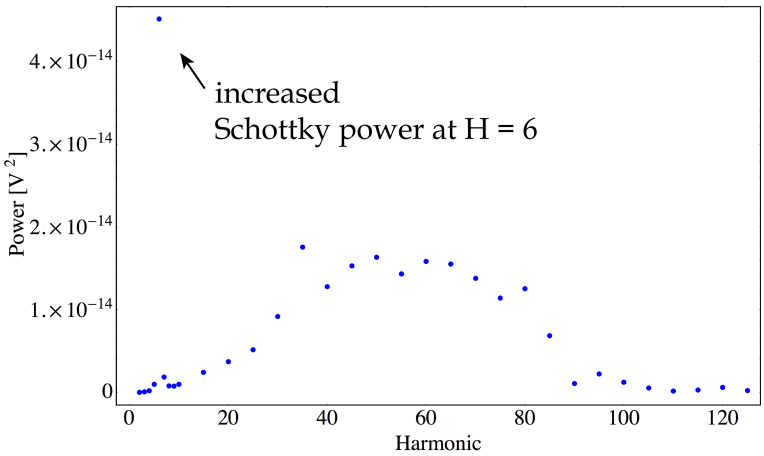

Figure 3.11: *Harmonic spectrum of the $^{12}C^{6+}$ ion beam, measured with one strip line of the Schottky pick-up and the NF 50 Ω amplifier.*

The power of the Schottky bands was corrected for the amplification and the damping of the cable and plotted against the harmonic number n. The function that was used to fit this data was described in chapter 2, equation (2.47):

$$P(n) = \kappa^2 \frac{4 f_0 I Q R^2}{1 + 4\pi^2 n^2 f_o^2 C^2 R^2} \left(1 - \cos(n 2\pi \frac{L}{c_0})\right) \tag{3.20}$$

The values for the input resistance of the amplifier $R = 50$ Ω and the capacity of the pick-up and amplifier $C = 68$ pF are all known, as are the length of the pick-up L and the circumference of the TSR c_0. The measurement was carried out with a 20 μA carbon beam with the charge $Q = 6 \cdot e^+$ and the revolution frequency $f_0 = 512.4$ kHz The data was fitted with the remaining fit parameter κ which was then compared to the theoretical value

$$\kappa_{theo} = \frac{\text{width of one strip line}}{\text{circumference of tube}} \approx 0.08\ . \tag{3.21}$$

The κ obtained by the data fit is $\kappa = 0.33$.

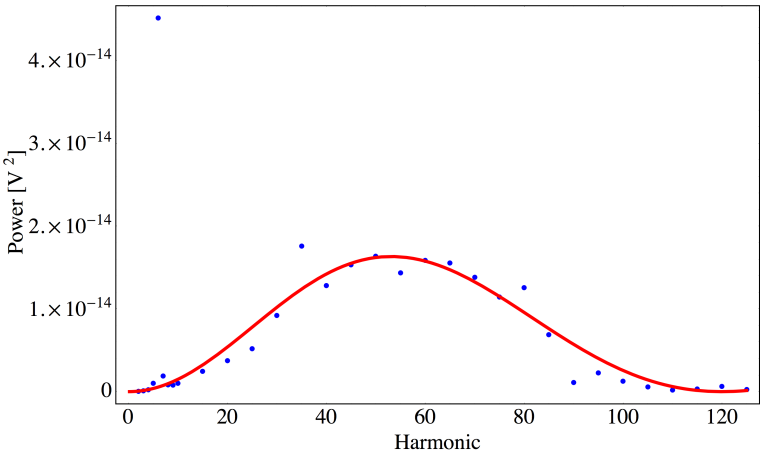

Figure 3.12: *Harmonic spectrum of the $^{12}C^{6+}$ ion beam, measured with one strip line of the Schottky pick-up and the NF 50 Ω amplifier including the fit through the data points.*

The ratio of the κ obtained through the data fit and the theoretical value κ_{theo} is:

$$V = \frac{\kappa}{\kappa_{theo}} \approx 4.13 \tag{3.22}$$

As can be seen in figure 3.12, the theory accurately describes the characteristics of the harmonic spectrum. The value for the κ that we obtained through the measurement, however, is larger than the theoretical value. That could be explained by the fact that the Schottky pick-up is not a closed tube. A larger voltage could be induced on the conductive strip lines of the pick-up, as the sides of the strip line also pick up some signal from the ion beam.
At the harmonic number $n = 6$ an increased Schottky power is visible (*see figure* 3.11), which can be described by the interaction of the stored ion beam with the rf-resonator, whose eigenfrequency was set to $6 \cdot f_0$. This will be further discussed in section 3.2.4.

The measurement was repeated with the Miteq preamplifier. Since there are four identical Miteq preamplifiers available, it was possible to carry out another measurement using all four strip lines of the Schottky pick-up. The fit function that was used is the same as in equation 3.20.
The fit values that were obtained through the data fit, κ_{1SL} for the measurement with one strip line and κ_{4SL} for the measurement with all four strip lines, are:

$$\kappa_{1SL} = 0.253 \qquad \text{and} \qquad \kappa_{4SL} = 0.495 \tag{3.23}$$

The signals from the four strip lines are combined with a hybrid that adds the individual

power signals. The ratio between the power signals is given by the ratio of κ^2_{4SL} and κ^2_{1SL}:

$$r = \frac{\kappa^2_{4SL}}{\kappa^2_{1SL}} = 3.89 \tag{3.24}$$

which comes very close to the expected value of $r = 4$.
The theoretical value for κ_{4SL} is given by

$$\kappa_{4SL,theo} = \frac{4 \cdot \text{width of one strip line}}{\text{circumference of tube}} \approx 0.32 \,, \tag{3.25}$$

so the ratio between the theoretical and the experimental value is:

$$V = \frac{\kappa_{4SL}}{\kappa_{4SL,theo}} \approx 1.55 \tag{3.26}$$

As with the measurement with one strip line and the NF 50 Ω amplifier, this is slightly larger than expected. This could again be explained by a larger voltage being induced on the sides of the strip lines, as the pick-up is not a closed tube.

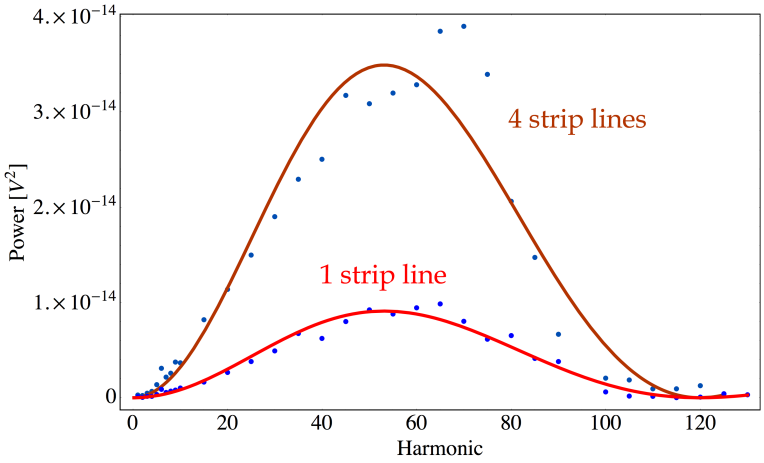

Figure 3.13: *Schottky harmonic spectra, measured with one and four strip lines of the Schottky pick-up, using four identical Miteq amplifiers.*

The measurement was once more repeated with the NF 1 MΩ amplifier. The fit function is the same as before, the only difference being the input resistance of the amplifier, now $R = 1$ MΩ, and the added input capacitance of approximately 50 pF, which results in an overall capacitance of $C = 118$ pF.
As can be seen in figure 3.14, the fit does not quite match the data points. There are several increases of the Schottky power along the harmonic spectrum.
These increases can be explained by the pick-up not being a pure capacitance at higher frequencies, as was assumed in the theory, but also an inductance. This causes the pick-up to be resonant and have self-oscillations, increasing the Schottky power at certain

frequencies. This could also explain the slight increases in power in the measurement with the NF 50 Ω amplifier that can be seen at the 35^{th} harmonic in figure 3.12.

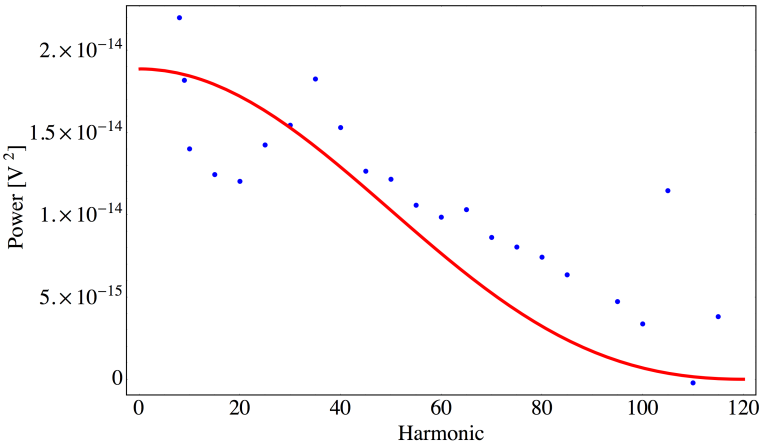

Figure 3.14: *Schottky harmonic spectrum measured with one strip line of the Schottky pick-up and the NF 1 MΩ amplifier including the fit through the data points.*

The κ that was obtained through the fit is $\kappa = 0.22$. This time the ratio of measured and theoretical κ is:

$$V = \frac{\kappa}{\kappa_{theo}} \approx 2.8 \; . \tag{3.27}$$

This deviation from the values for the NF 50 Ω amplifier could be explained by the fact that the NF 1 MΩ amplifier had to be repaired before and the input impedance might therefore not be 1 MΩ anymore. Also, the input capacitance of the preamplifier is only approximately known and might also have been changed during the reparations. An input capacitance of $C = 106$ pF would result in the same ratio $V = 4.13$ as the measurement with the NF 50 Ω amplifier.

3.2.2 Measurement with the AM12 pick-up

The AM12 pick-up is another pick-up that was used to measure the Schottky harmonic spectrum of a $^{12}C^{6+}$ ion beam with 50 MeV energy and a current of $I = 20$ μA.
The harmonic spectrum that was measured with the NF 50 Ω amplifier is shown in figure 3.15.
We can see that there is an increase of the Schottky power in the Schottky bands around the 180^{th} harmonic. This increase is even more pronounced in the harmonic spectrum that was measured with the NF 1 MΩ amplifier (*see figure* 3.17). Those increases are

most probably due to self-oscillations of the system, which could already be observed in the measurements with one strip line of the Schottky pick-up and the NF 1 MΩ amplifier (*see section* 3.2.1, *figure* 3.14). The increased Schottky powers at the harmonics around the self-oscillation were disregarded for the fit, which was performed with the fit function in equation (3.20).
However, as can be seen, the fit does also not match the minimum of the data points around the 300^{th} harmonic. As the position of the minimum of the fit function is defined by the length of the pick-up, another fit was made, this time using the length as a second fit parameter. The result is shown in figure 3.16.

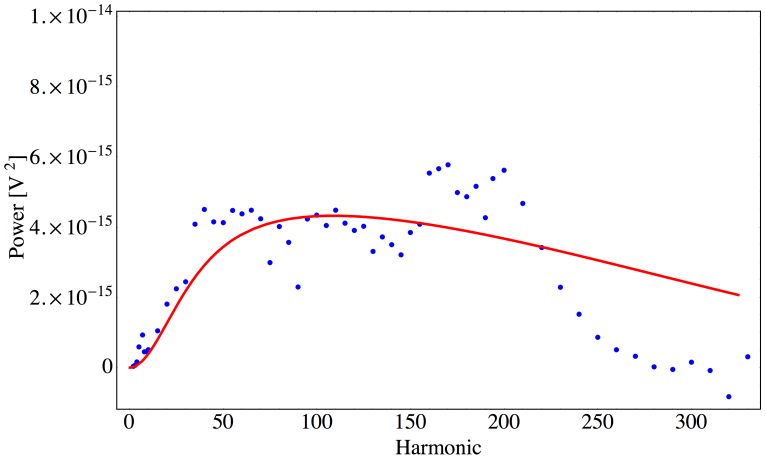

Figure 3.15: *Harmonic spectrum measured with the AM12 pick-up and the NF 50 Ω amplifier. The pick-up length of 8.6 cm was used in the fit, but does not accurately describe the minimum of the spectrum.*

The second fit yielded a length of $L = 16.2$ cm and $\kappa = 0.55$. This shows that the length that best represents the data exceeds the length of the actual pick-up. Also, the theoretical value is $\kappa_{theo} = 1$ for a closed tube, resulting in a ratio:

$$V = \frac{\kappa}{\kappa_{theo}} \approx 0.55 \; . \tag{3.28}$$

The measured κ is too small for a closed tube. From this, we can conclude that there is a required minimum length that a Schottky pick-up needs to have for the theory of Schottky diagnostics to apply. More thoughts on the pick-up length follow in section 3.3.
The measurement that was carried out with the NF 1 MΩ amplifier yielded a length of 21.1 cm and $\kappa = 0.36$,

$$V = \frac{\kappa}{\kappa_{theo}} \approx 0.36 \; . \tag{3.29}$$

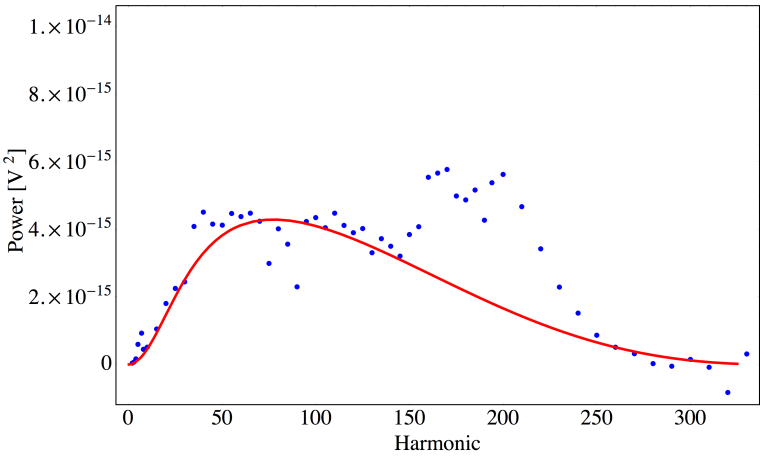

Figure 3.16: *Harmonic spectrum measured with the AM12 pick-up and the NF 50 Ω amplifier. The length was used as a second fit parameter. The increased values for the Schottky power around the 180^{th} harmonic were not considered for the data fit.*

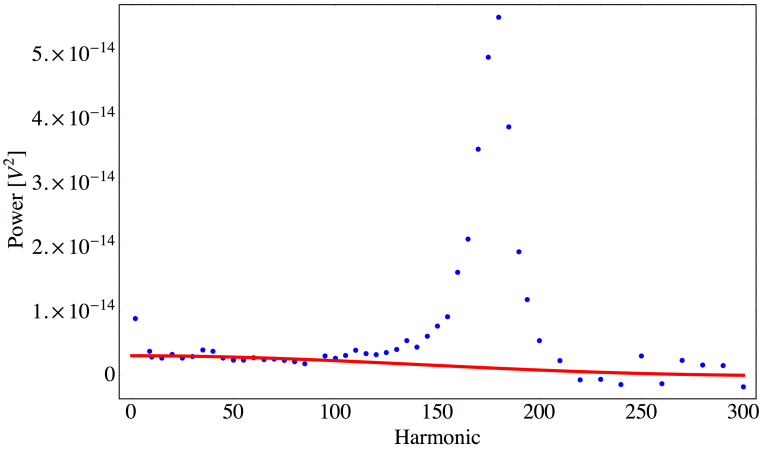

Figure 3.17: *Harmonic spectrum measured with the AM12 pick-up and the NF 1MΩ amplifier. The increase in Schottky power due to self-oscillations around the 180^{th} harmonic is very pronounced.*

The deviation from the value of κ obtained through the fit of the measurement with the NF 50 Ω amplifier could be explained by the input resistance and capacitance of the NF 1 MΩ amplifier varying from the data provided by the manufacturer, due to the reparation of the amplifier. This was already observed in section 3.2.1, while discussing the results from the fit of the measurement with one strip line of the Schottky pick-up and the NF 1 MΩ amplifier. If we assume an input capacity of $C = 106$ pF, as was suggested in section 3.2.1, we obtain $\kappa = 0.46$, which comes closer to the value from the fit with the

NF 50 Ω amplifier, indicating that the NF 1 MΩ amplifier does indeed have a higher input capacitance than 50 pF.
The lengths from the two fits could differ because the increase in the Schottky power due to the self-oscillation of the system was much higher in the measurements with the NF 1 MΩ amplifier and data points for more harmonics had to be discarded for the fit. This probably resulted in the different values for the pick-up length.
The increase in Schottky power around the 180^{th} harmonic is more pronounced in the measurement with the NF 1 MΩ, because a preamplifier with an input resistance of 1 MΩ does not dampen the self-oscillation of the pick-up as much as an amplifier with $R = 50\ \Omega$.

3.2.3 Width of the Schottky bands and momentum spread

Another important value from the Gaussian fit function in equation (3.19) is the width of the distribution, σ, for each Schottky band. This width was plotted against the harmonic number. The results from the measurement using four strip lines of the Schottky pick-up and the Miteq preamplifiers are shown in figure 3.18.

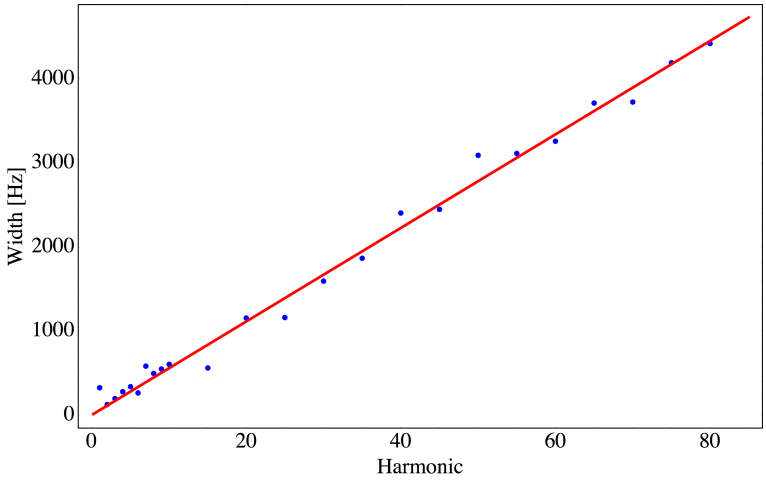

Figure 3.18: *The width of the Schottky bands measured with four strip lines of the Schottky pick-up and Miteq amplifiers plotted against the harmonic number.*

The data was fitted with the function

$$\sigma_n = \alpha \cdot n \ . \tag{3.30}$$

Using the fit parameter α and equation (2.49), the relative momentum spread is given by

$$\frac{\Delta p}{p} = \frac{1}{\eta}\,\frac{\Delta f_n}{f_n} = \frac{1}{\eta}\,\frac{\alpha}{f_0} \qquad \text{with} \quad \Delta f_n = \sigma_n \ . \tag{3.31}$$

The fit parameter that was obtained from the data fit is $\alpha = 55.6$ Hz, resulting in a relative momentum spread of $1.2 \cdot 10^{-4}$ for the electron cooled, 50 MeV $^{12}C^{6+}$ ion beam at a current of $I = 20$ μA.

3.2.4 Increase of the Schottky power at the eigenfrequency of the resonator

For acceleration and deceleration of non-relativistic heavy ions on closed orbits in the TSR, variable frequency ferrite loaded resonators are used. The resonance frequency variation is realized by changing the ferrite permeability [5]. The interaction with the resonator causes a longitudinal density modulation of the ion beam, which produces an increase in the signal at the associated frequency. The more precisely the resonator is matched to the harmonic, the higher the increase.
The increase in the Schottky power at the 6^{th} harmonic seen in figure 3.11 is caused by the interaction of the ion beam with the rf-resonator, where the eigenfrequency of the resonator is set to a multiple n of the revolution frequency f_0, in this case $n = 6$.
The resonator eigenfrequency can be adjusted by changing the magnetization of the ferrites. Figure 3.19 shows the Schottky power of the first ten harmonics with the ferrite magnetization set to 58 A. This resulted in an eigenfrequency of the resonator of $5 \cdot f_0$, which caused the fifth harmonic in the harmonic Schottky spectrum to be increased. A ferrite magnetization of 65 A changes the eigenfrequency of the resonator to $6 \cdot f_0$ and increases the sixth harmonic of the harmonic power spectrum, which can be seen in figure 3.20.

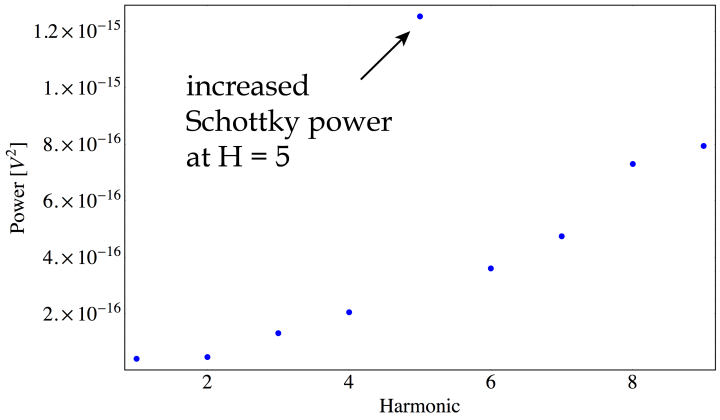

Figure 3.19: *Harmonic spectrum of a $^{12}C^{6+}$ ion beam, measured with one strip line of the Schottky pick-up and the NF 50 Ω amplifier. The Schottky power at n = 5 is increased due to interaction with the rf-resonator.*

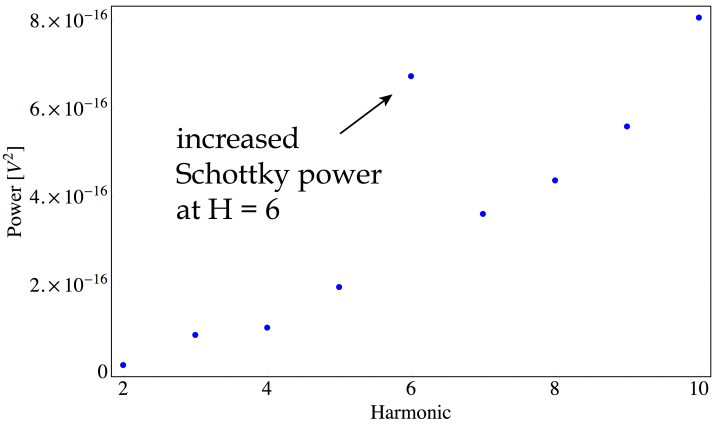

Figure 3.20: *Harmonic spectrum of a $^{12}C^{6+}$ ion beam, measured with one strip line of the Schottky pick-up and the NF 50 Ω amplifier. The Schottky power at n = 6 is increased due to interaction with the rf-resonator.*

3.3 The Schottky pick-up length

As the results from the measurements with the AM12 pick-up indicate (*see section* 3.2.2), equation (3.20), which describes the Schottky power, does not accurately describe the experimental results for a pick-up of small length.

In the theory deriving equation (3.20), it was assumed that the ion current of an ion with the charge Q at the pick-up can be described by a δ-Pulse $I(t) = Q\,\delta(t - t_0)$. In a pick-up with the length L and the capacity C, such an ion current will produce the voltage:

$$U = \frac{\int_{t_0}^{t_0+\Delta t} I(t')\mathrm{d}t'}{C} = \frac{Q}{C} \qquad \text{with} \quad \Delta t = \frac{L}{v} \tag{3.32}$$

with v being the velocity of the ion.

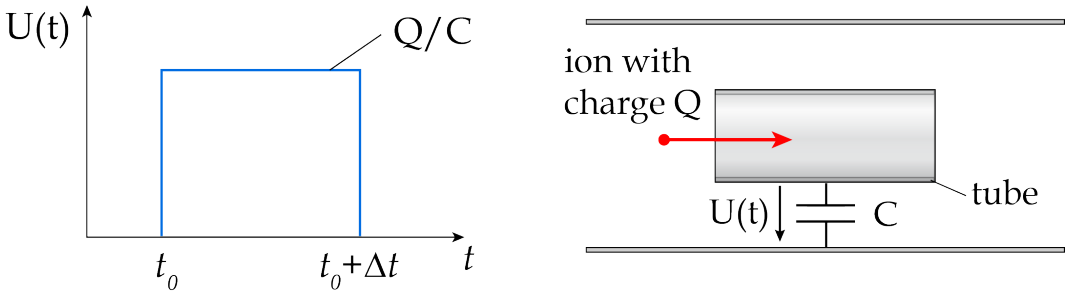

Figure 3.21: *The voltage signal produced by a single ion with the charge Q in a pick-up with the capacity C in our simplified model.*

However, it takes a certain rise time t_{rise} for the ion to induce a voltage in the pick-up. If the pick-up length is too small, the ion will already have left the pick-up before this rise time has passed and the signal will not reach its maximum.

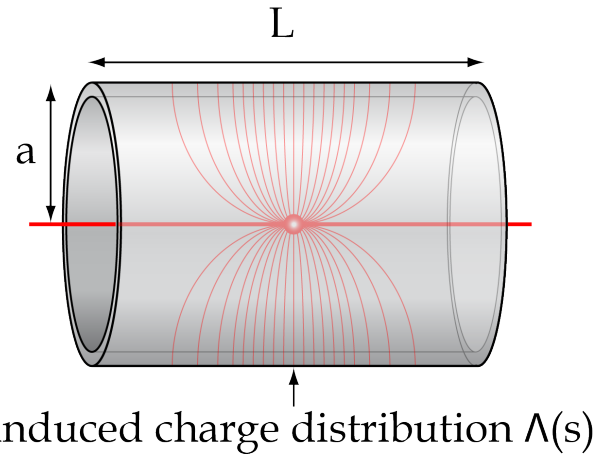

Figure 3.22: *The charge on the outside of the pick-up, influenced by the ion, can be described by a Gaussian charge distribution $\Lambda(s)$. The width σ of this distribution depends on the velocity of the ion and the radius of the pick-up tube a.*

The rise time of the pick-up signal can be estimated by considering an ion moving through a tube with the radius a and length L. The ion induces an image charge on the inside of the pick-up wall that is equivalent to its negative charge. Because of charge conservation, the outside surface of the pick-up will have a charge distribution $\Lambda(s)$, the total charge of which is equal to the ion charge Q (with s being the position along the pick-up). For $L \gg a$, this charge distribution has a Gaussian profile with [6]:

$$\sigma = \frac{a}{\gamma\sqrt{2}}, \qquad \text{with} \quad \gamma = \frac{1}{\sqrt{1-\frac{v^2}{c^2}}} \qquad \text{and} \quad \int_0^L \Lambda(s)\mathrm{d}s = Q \tag{3.33}$$

where σ is the width of the distribution.
If an ion enters the pick-up, the pick-up voltage will increase with the rise time:

$$t_{rise} \approx \frac{\sigma}{v}\,. \tag{3.34}$$

To get the maximum induced voltage $U = Q/C$ on the pick-up, the rise time t_{rise} must be much smaller than the time that it takes for the ion to pass through the pick-up, Δt.

$$\Delta t \gg t_{rise} \tag{3.35}$$

$$\frac{L}{v} \gg \frac{\sigma}{v} = \frac{a}{\sqrt{2}\gamma v} \tag{3.36}$$

This means that the length of the pick-up tube must be much greater than the radius $L \gg a$.

In the case of the measurements that were conducted with the AM12 pick-up ($a = 10$ cm, $L = 8.6$ cm), the condition $L \gg a$ is not fulfilled, resulting in a much smaller Schottky power than expected with equation (3.20). This was verified by the measurements discussed in section 3.2.2, which show that the power measured with the AM12 pick-up is only about 50% of what was expected.

4. Outlook and summary

In this chapter the conclusions from the measurements are combined to model the pick-up that will be used in the Cryogenic Storage Ring (CSR), which is currently under construction at the MPIK. Also, it is described how the signal can be increased by using a resonant LC circuit to measure the Schottky niose.

As was discussed in chapter 3.3, the pick-up has to have a certain length. This was also verified by the results from the measurements with the AM12 pick-up (*see section* 3.2.2). The Schottky pick-up that will be used in the CSR will have a radius of $a = 5$ cm and the condition $L \gg a$ is fulfilled if a pick-up length of

$$L = 7 \cdot a = 35\,\text{cm} \tag{4.1}$$

is chosen, corresponding to 1 % of the circumference of the CSR, which will be 35 m once it is completed [7].

To increase the signal of an ion passing through the pick-up tube, an inductance will be connected parallel to the pick-up capacity, forming a resonant LC circuit (*see figure* 4.1). As was described in chapter 2, equation (2.37), the spectrum of the current flowing into the circuit is given by

$$\Delta\hat{I}_i(\omega_n) = \frac{2\sqrt{2}Q}{T}\sqrt{1-\cos(\omega_n\frac{L}{v})} \tag{4.2}$$

The voltage of a single ion at the resonance frequency ω_n of the LC circuit is given by

$$\hat{U}_i(\omega_n) = \frac{Q_W}{\omega_n C}\frac{2\sqrt{2}Q}{T}\sqrt{1-\cos(\omega_n\frac{L}{v})} \tag{4.3}$$

with Q_W being the quality factor (Q - factor) of the LC circuit.

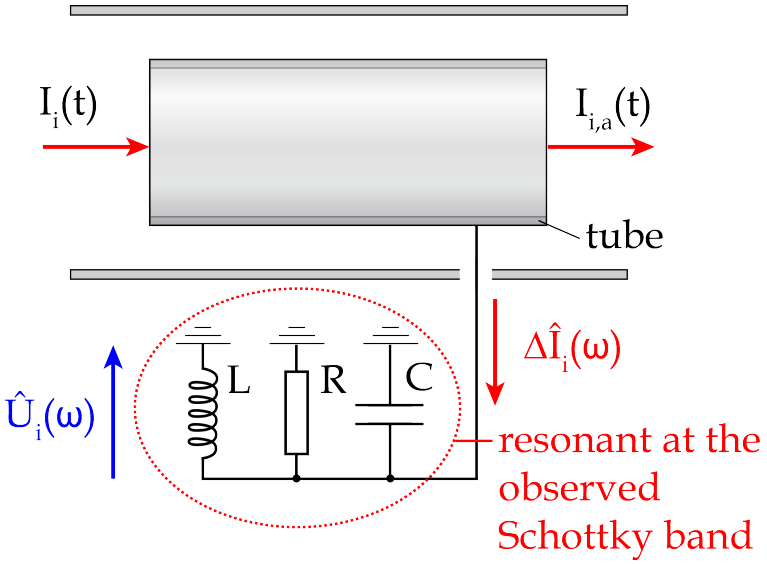

Figure 4.1: *Sketch of a Schottky pick-up and the resonant LC circuit used to increase the Schottky power. C describes the capacity of the pick-up, R describes the losses of the circuit including the input resistance of a preamplifier and L is an inductance that is chosen so the circuit is resonant at the observed Schottky band.*

Now the signal of a single proton stored in the CSR with an energy of $E = 300$ keV, which corresponds to a revolution frequency of about $f_0 = 216$ kHz, will be estimated. In the frequency range of 200 kHz - 1 MHz an LC circuit can be built with a Q-factor of $Q_W \approx 1000$, if the circuit is cooled down to a temperature of about 4 K. For the capacitance we assume $C = 100$ pF; the circumference of the CSR is $c_0 = 35$ m and the length of the Schottky pick-up $L = 35$ cm. As is shown in figure 4.2, a proton induces a maximum voltage of 30 nV at low harmonic numbers $H = 1$ - 10, which corresponds to frequencies in the range of 200 kHz - 2 MHz.

In summary, it can be said that the signals of a long enough pick-up can be accurately described by the theory of Schottky diagnostics. Even though the values for the fit parameter κ were larger than expected for the measurements with the strip lines of the Schottky pick-up, the characteristics of the harmonic Schottky spectra match the theory. Deviations from the theory can be explained by increased signals due to self-oscillations in the system.
If the pick-up is too short, the electric charge of the ion beam will not be entirely induced on the pick-up wall and the signals are smaller than they should be. The measurements that were performed with one and four strip lines of the Schottky pick-up show that the

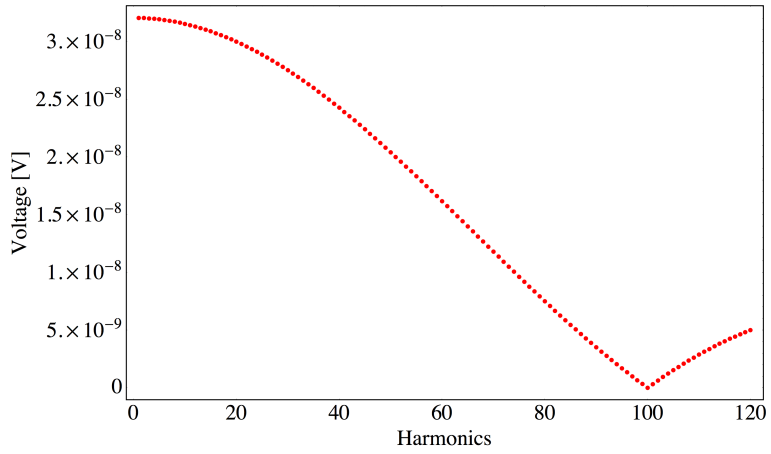

Figure 4.2: *The harmonic spectrum of a single proton with the energy $E = 300$ MeV, measured with a resonant circuit with Q - factor $Q_W = 1000$ and a pick-up tube with the length $L = 35$ cm.*

signal depends on the area around the beam that is covered by the pick-up. This means that a closed tube, which will be in use in the CSR, is an ideal Schottky pick-up.

Experiments at the CSR will be carried out not only with protons, but also with heavy ions. These ions will be much slower than the protons, having revolution frequencies of about 20 kHz. Using the same resonant circuit and measuring in the same frequency range as with the protons, this means measuring at high harmonics. For example, if the circuit is resonant at about 2 MHz, for a proton with an energy of $E = 300$ keV this means measuring at a harmonic number of $n = 10$, whereas for a slow ion, this corresponds to a harmonic number of $n = 100$. As the experiments demonstrated, the theory of Schottky noise diagnostics is accurate even for high harmonic numbers of the revolution frequency, which ensures that Schottky diagnostics for slow ions at high harmonics will be possible.

List of Figures

Bibliography

[1] E. Jaeschke, D. Krämer, W. Arnold, G. Bisoffi, M. Blum, A. Friedrich, C. Geyer, M. Grieser, D. Habs, H. Heyng, B. Holzer, R. Ihde, M. Jung, K. Matl, R. Neumann, A. Noda, W. Ott, B. Povh, R. Repnow, F. Schmitt, M. Steck, and E. Steffens in *Proceedings of the first European Particle Accelerator Conference, Rome 1988*, p. 365, World Scientific, Singapore, 1989.

[2] D. Boussard, "Schottky noise and beam transfer function diagnostics," in *Cern Accelerator School, Advanced Accelerator Physics, Oxford, England, 1985, Proceedings* (S. Turner, ed.), vol. II, CERN, Geneva, 1987.

[3] K. Lange and K.-H. Löcherer, eds., *Meinke/Gundlach - Taschenbuch der Hochfrequenztechnik*. Springer Verlag Berlin Heidelberg New York Tokyo, fourth ed., 1986.

[4] H.-G. Unger, *Elektromagnetische Wellen auf Leitungen*. Dr. Alfred Hüthig Verlag Heidelberg, 1980.

[5] M. Blum, M. Grieser, E. Jaeschke, D. Krämer, and S. Papureanu, "A new type of acceleration cavity for the Heidelberg test storage ring TSR," in *EPAC 1990, Nice*, 1990.

[6] A. Hoffmann, "Dynamics of beam diagnostics," in *Cern Accelerator School, Beam Diagnsotics, Dourdan, France, 2008, Proceedings* (D. Brandt, ed.), vol. V, CERN, Geneva, 2009.

[7] R. von Hahn, K. Blaum, J. C. López-Urrutia, M. Froese, M. Grieser, M. Lange, F. Laux, S. Menk, J. Varju, D. Orlov, R. Repnow, C. Schröter, D. Schwalm, T. Sieber, J. Ullrich, A. Wolf, M. Rappaport, D. Zajfman, X. Urbain, and H. Quack, "The cryogenic storage ring project at Heidelberg," in *Proceedings 2008 EPAC08, Genoa, Italy*, p. 394, 2008.

Danksagung

An dieser Stelle möchte ich gerne all den Leuten danken, die mir bei der Erarbeitung meiner Bachelorarbeit geholfen haben.

Mein erster herzlicher Dank richtet sich an Dr. Manfred Grieser, für seine engagierte und lehrreiche Betreuung während meiner Arbeit, ausführliche Erklärungen und die gründlichen Korrekturen während des Schreibens. Ganz herzlich möchte ich mich auch bei Felix Laux bedanken, für die tatkräftige Unterstützung bei vielen Messungen, Mathematica Tipps, die mir viel Zeit und Nerven gespart haben und zahlreiche beantwortete Fragen.

Besonders bedanken möchte ich mich auch bei Prof. Andreas Wolf, der mir ermöglicht hat, meine Bachelorarbeit in seiner Arbeitsgruppe zu schreiben und für seine kritische Durchsicht der Arbeit. Desweiteren danke ich Prof. Klaus Blaum für die Übernahme der Zweitkorrektur dieser Arbeit.

Ein weiterer Dank gilt meinen beiden Bürokollegen Wieland Reis und Arthur Schönhals für die Tipps beim Schreiben, sowie allen weiteren Mitgliedern der Arbeitsgruppe für eine tolle Arbeitsatmosphäre.

Den Operateuren des TSR und der Beschleunigeranlagen möchte ich für ihre Unterstützung während der Strahlzeiten danken, insbesondere Kurt Horn, der immer zur Stelle war und geholfen hat, wenn etwas nicht funktionierte.

Außerdem geht ein herzlicher Dank an Helen Morrison, die mich bei der englischen Grammatik und Rechtschreibung vor einigen Fehlern bewahrt hat.

Ein ganz besonderer Dank gilt meiner Familie, die mir mit ihrer finanziellen Unterstützung dieses Studium ermöglichen und mit ihrer moralischen Unterstützung immer den Rücken gestärkt haben.

Erklärung:

Ich, Frederike Schmitz, versichere hiermit, dass ich diese Arbeit selbständig verfasst und keine anderen als die angegebenen Quellen und Hilfsmittel benutzt habe.

Heidelberg, den .....

.....
(Unterschrift)